



# IJRASET

International Journal For Research in  
Applied Science and Engineering Technology



---

# INTERNATIONAL JOURNAL FOR RESEARCH

IN APPLIED SCIENCE & ENGINEERING TECHNOLOGY

---

**Volume:** 10    **Issue:** II    **Month of publication:** February 2022

**DOI:** <https://doi.org/10.22214/ijraset.2022.40284>

[www.ijraset.com](http://www.ijraset.com)

Call:  08813907089

E-mail ID: [ijraset@gmail.com](mailto:ijraset@gmail.com)

# Synthesis and the Study of Mechanism of Perovskite Formation of Pb (Fe<sub>0.5</sub>Nb<sub>0.5</sub>)O<sub>3</sub> Ceramics

V. Rathod

**Abstract:** Lead iron neobate Pb(Fe<sub>0.5</sub>Nb<sub>0.5</sub>)O<sub>3</sub> ceramics were prepared by using B-site precursor method. The formation of perovskite phase and microstructure are reported. The formation of B-site precursor and perovskite formation mechanism were studied by using X-ray diffraction and thermal analysis.

**Keywords:** B-site precursor, pyrochlore, perovskite phase, PFN Ceramic

## I. INTRODUCTION

The ferromagnetic ceramics are smart materials which shows two or more types of physical states (i.e, a ferromagnetic, ferroelectric, ferroelastic, ferrotoroid state) [1-4]. PFN is one of the material belonging to this group. The PFN ceramic has perovskite structure with general formula A(B<sub>1-x</sub>B<sub>x</sub>)O<sub>3</sub> where Pb<sup>2+</sup> in A-site, Fe<sup>3+</sup> and Nb<sup>5+</sup> in B-site.

Lead iron neobate (PFN) have been synthesized by many techniques and methods e.g, wet chemical processing routes such as sol-gel, semi wet hydroxide route and coprecipitation, molten salt synthesis, high energy ball milling e.t.c, [5-8]. In the present paper the B-site precursor method was used to synthesize PFN ceramics and the formation of perovskite phase were presented.

## II. EXPERIMENTAL SETUP

### A. Sample Preparation

The B-site precursor method is employed for the preparation of the ceramic Lead Iron Niobate (PFN). The starting materials used in this method are PbO, Nb<sub>2</sub>O<sub>5</sub> and Fe<sub>2</sub>O<sub>3</sub>. B-site precursor method is a two- step calcination method. In this method the B-site oxides Fe<sub>2</sub>O<sub>3</sub> and Nb<sub>2</sub>O<sub>5</sub> were mixed stoichiometrically in ethanol medium by ball milling for 1hr. The slurry was dried and calcined at 1000°C for 4 hr. After calcination the molten mass was slowly cooled to R.T and the cooled solid FeNbO<sub>4</sub> was crushed to fine powder by using Pestle and Mortar. The stoichiometric amount of PbO and precursor FeNbO<sub>4</sub> was mixed in ethanol medium by ball milling for 2 hr and was dried. The second stage of calcination was carried out at 750°C for 2 hr. The calcined powder was crushed and ground finely. 2 gm of PbO excess was added to the calcined powder to compensate for the PbO loss and ball milled for 1hr. The powder was pressed in to pellet of 10-12 mm diameter and 1-2 mm thickness by applying pressure of 70 M Pa. The pellets were sintered at 1000°C for 2 hr in a closed alumina crucible. The sintered pellets were checked by X-ray diffraction for the formation of perovskite phase.

### B. X-ray Diffraction (XRD)

The X-ray diffraction technique was employed for determining the phase purity and lattice parameter calculation.

#### X-ray characterization

Following calcination as well as sintering, the formation of the various phases was checked by their X-ray diffraction patterns. The X-ray patterns were recorded on a computerized Phillips (1070 model) diffractometer with a scanning speed of 1°/min using CuK $\alpha$  radiation. The percentage of perovskite phase was calculated using the following equation [2].

$$\%Perovskite = \frac{I_{110}}{(I_{110} + I_{222})} \times 100$$

where  $I_{110}$  and  $I_{222}$  are the areas under the major peaks (110) and (222) of perovskite and pyrochlore phases respectively.

### C. Thermogravimetry and Differential Thermal Analysis (TG and DTA)

The TG/DTA curves were acquired from an automated simultaneous thermal analysis (Polymer Laboratories, STA/1500). About 20mg of sample was taken and heated at a rate of 5°C /minute up to about 1000°C.

#### D. Scanning Electron Microscopy (SEM)

The powder morphology of a heat-treated and the fractured surface of a sintered pellet (to measure the grain size) were investigated using Leica Cambridge Stereoscan S-360 scanning electron microscope (SEM). Conducting gold was sputtered on the sample to avoid charging at the sample surfaces. They were examined under SEM and selected areas were photographed. The grain size was calculated using linear intercept technique and the average grain size was calculated by the following equation [9],

$$\text{Grain size} = 1.56 C / [M N]$$

Where, C is the length of the test line, N is the number of intercepts and M is the magnification calculated from the reference scale printed on the micrograph.

### III. RESULTS AND DISCUSSION

#### A. XRD Studies

The XRD studies were carried out for calcined PFN. Fig 3.1 (a) shows the XRD pattern for PFN calcined at 750°C for 2 hr. Fig 3.1(b) shows JCPDS pattern for PFN. From fig 3.1(a) and 3.1(b) it is clear that there are additional peaks in the experimental XRD pattern for PFN, and these peaks are due to pyrochlore phase. Percentage of individual phase was calculated, by comparing 100% peak intensities of the perovskite peak and pyrochlore peak. The % of perovskite formed in the calcined powder was found to be 73%. Therefore, the remaining 27% corresponds to pyrochlore phase. Fig 3.1(c) shows the XRD pattern for PFN sintered at 1000°C for 2 hr. From JCPDS pattern for PFN fig 3.1(b) and experimental XRD pattern for sintered PFN, it is clear that additional peaks present before sintering are removed and this confirms the formation of single phase perovskite PFN.

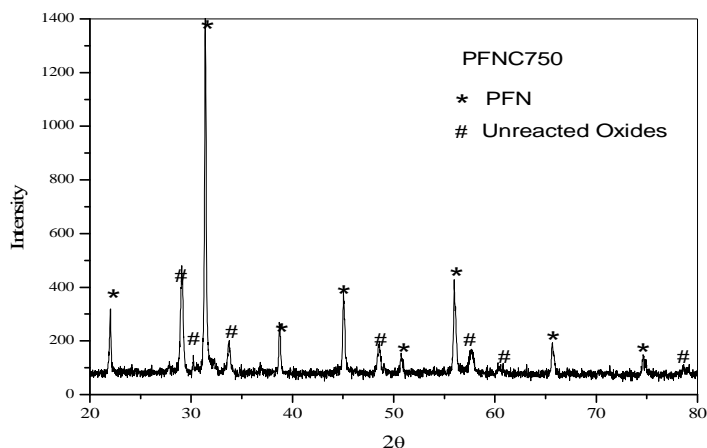


Fig 3.1(a): XRD for PFN Calcined at 750 for 2 hr.

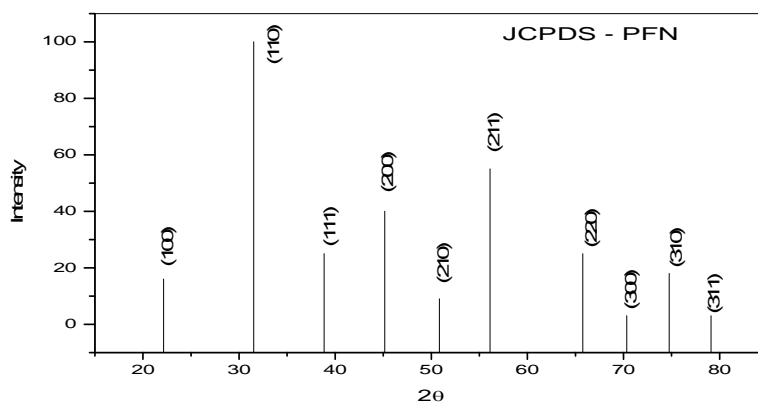


Fig 3.1(b): JCPDS data for PFN.

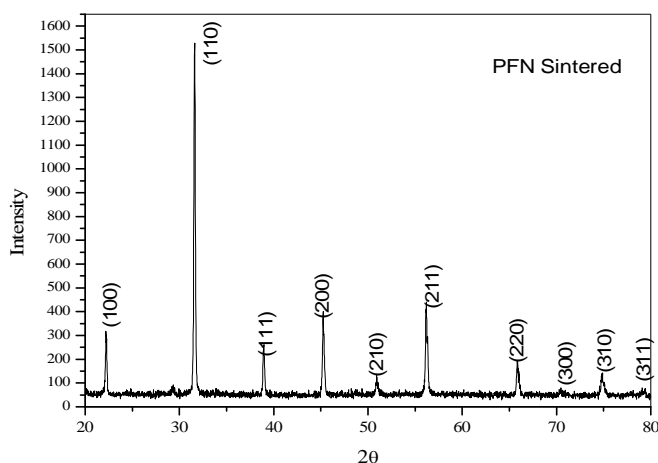


Fig 3.1(c): XRD for PFN Sintered at 1000°C for 2 hr.

**B. TG/DTA Studies**

TG/DTA studies were done during heating and cooling of the sample to examine the weight changes and the phase stability of the powders (PbO, Nb<sub>2</sub>O<sub>5</sub>, Fe<sub>2</sub>O<sub>3</sub>, FeNbO<sub>4</sub>+PbO and PFN after calcination). These results are shown in figures 3.2(a) to 3.2(e). Fig 3.2(a) shows the TG/DTA curve for PbO. DTA curve shows two endotherms. The endotherm at ~300°C is due to the loss of CO<sub>2</sub> and the endotherm at ~500°C is due to the formation of Pb<sub>3</sub>O<sub>4</sub>. In fig 3.2(a) DTA curveshows three phases and two exotherms. The three phases are PbO, Pb<sub>3</sub>O<sub>4</sub> and PbO. The exotherm at ~300°C corresponds to the phase transition from PbO to Pb<sub>3</sub>O<sub>4</sub>. The exotherm at ~550°C corresponds to the phase transition from Pb<sub>3</sub>O<sub>4</sub> to PbO. Above 550°C this Pb<sub>3</sub>O<sub>4</sub> transforms in to PbO. The TG curve in fig 3.2(a) shows the weight loss corresponding to the endotherm at ~300°C due to loss of CO<sub>2</sub>. And the weight gain corresponding to the endotherm at ~500°C is due to the formation of Pb<sub>3</sub>O<sub>4</sub> from PbO. Fig 3.2(b) shows TG/DTA curves for Nb<sub>2</sub>O<sub>5</sub>. From DTA curve we can infer that there is no change in phase for Nb<sub>2</sub>O<sub>5</sub>. Also from TG curve we can infer that there is no change in weight for Nb<sub>2</sub>O<sub>5</sub>. Fig 3.2(c) shows TG/DTA curve for Fe<sub>2</sub>O<sub>3</sub>. From TG and DTA curves we can infer that there is no change respectively, in weight and phase for Fe<sub>2</sub>O<sub>3</sub>. Fig 3.2(d) shows TG/DTA curves for the mixture FeNbO<sub>4</sub>+PbO. DTA curve shows three phases, two endotherms and two exotherms. The three different phases are FeNbO<sub>4</sub>+PbO, pyrochlore and perovskite phase. The endotherm at 300°C is due to loss of CO<sub>2</sub> and the endotherm at 500°C is due to the formation of pyrochlore. The exotherm at 300°C corresponds to the phase transition from FeNbO<sub>4</sub>+PbO to pyrochlore phase. The exotherm at ~550°C corresponds to the phase formation from pyrochlore to perovskite phase and at 750°C the phase transition completes relating to the formation of perovskite phase which agrees with a previous report [10]. The TG curve in fig 3.2(d) shows weight loss corresponding to the endotherm at ~300°C due to loss of CO<sub>2</sub> and the weight gain corresponding to the endotherm at ~500°C due to the formation of pyrochlore is not much as seen in fig 3.2(a). Fig 3.2(e) shows TG/DTA curves for PFN after calcination.

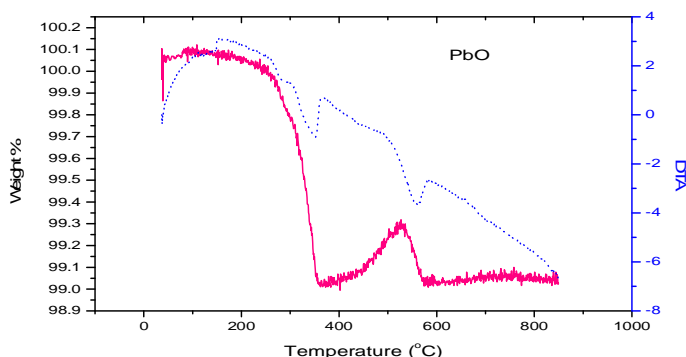


Fig 3.2(a): TG/DTA Curve for PbO.

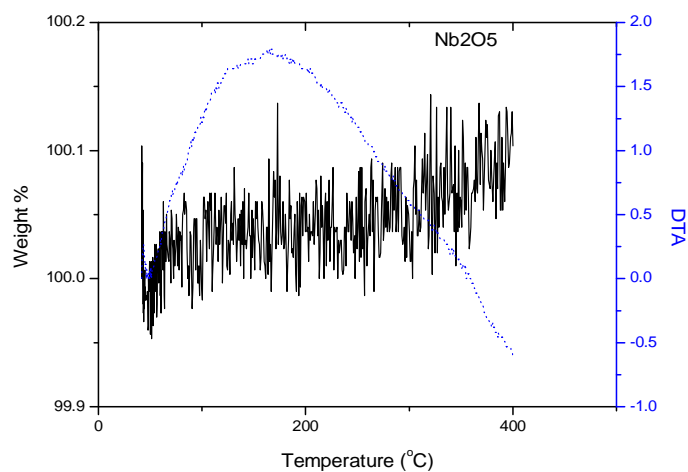


Fig 3.2(b): TG/DTA Curve for Nb<sub>2</sub>O<sub>5</sub>.

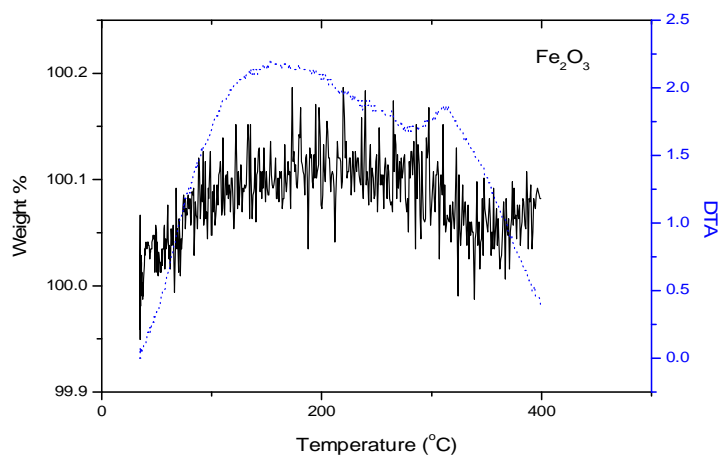


Fig 3.2(c): TG/DTA Curve for Fe<sub>2</sub>O<sub>3</sub>.

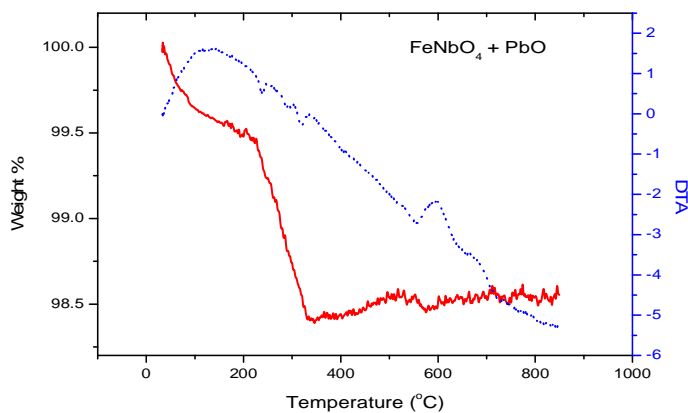


Fig 3.2(d): TG/DTA Curve for FeNbO<sub>4</sub>+PbO.



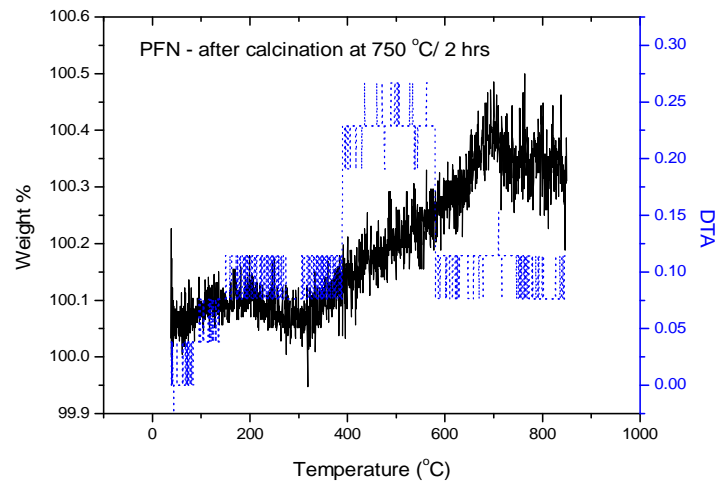


Fig 3.2(e): TG/DTA Curve for PFN.

### C. Scanning Electron Microscopy (SEM)

Fig 3.3(a) shows SEM for PFN sintered at 1000°C. Average grain size was found to be  $\sim 1.05\mu\text{m}$ . This value is in good agreement with the previous report [10].

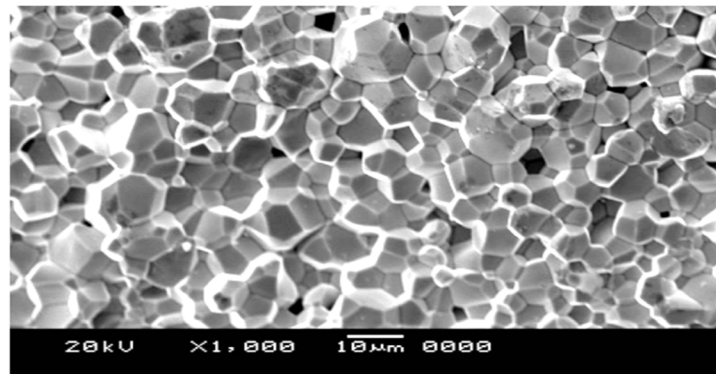


Fig 3.3(a) SEM image for PFN sintered at 1000°C.

## IV. CONCLUSION

Lead Iron Niobium Oxide PFN ceramic has been prepared by B-site precursor method. The weight changes during heating and cooling of the sample and the phase stability of the starting materials was examined. The formation of single phase perovskite was confirmed from XRD pattern. A well-established PFN phase of  $\sim 1.05\mu\text{m}$  in particle size was obtained which was confirmed from SEM.

## REFERENCES

- [1] D. Bochenek and P. Niemiec, Dielectric Properties of the PFN ceramics obtained different chemical-wet technology and sintering by hot pressing method, MATEC Web of Conferences, 242, 2018.
- [2] D. Khomskii, Physics, 2, 2009
- [3] H. Schmid, J. Phys. Condens. Matter, 20, 2008
- [4] M.H. Lente, J.D.S. Guerra, G.K.S. de Souza, B.M. Fraygola, C.F.V. Raigoza, D. Gareia, J.A. Eiras, Phys. Rev. B, 78, 2008
- [5] Y. Ch. Liou, Ch-Yu Shih, Ch-H. Yu, Jpn. J. Appl. Phys, 99, 1999
- [6] S. Ananta, N.W. Thomas, J. Eur. Ceram. Soc, 19, 1999
- [7] S.B. Majumder, S. Bhattacharyya, R.S. Katiyar, A. Manivannan, P. Dutta, M.S. Seehra, J. Appl. Phys, 99, 2006.
- [8] X. Gao, J. Xue, J. Wang, T. Yu, Z.X. Shen, J. Am. Ceram. Soc, 85, 2002.
- [9] M.V.Radhikarao, Thesis, MRC, IISC, Bangalore, 1998.
- [10] XingsenGaoJunminXue, and John Wang, J.Am.Ceram.Soc.85 565-72 (2002).



#### ABOUT THE AUTHOR

Dr. Vinodkumar Rathod is currently working as Assistant Professor of Physics at Government College (Autonomous) Kalaburagi. He has about 20 years of teaching experience including Undergraduate and Post graduate. He served as Chairman Department of Physics in GFGC Shahapur and Government College Kalaburagi. He Served as Chairman and Member of BOS and BOE (UG&PG) at Government College (Autonomous) Kalaburagi and BOE member at Gulbarga University Kalaburagi. He has published many Research articles in National and International Journals and presented Research papers in Regional, National Seminars. Completed one UGC Research Project.



Dr. Vinodkumar Rathod

E-mail: [vinodkumarsrathod@gmail.com](mailto:vinodkumarsrathod@gmail.com)

Cell: +91 9448586111



10.22214/IJRASET



45.98



IMPACT FACTOR:  
7.129



IMPACT FACTOR:  
7.429



# INTERNATIONAL JOURNAL FOR RESEARCH

IN APPLIED SCIENCE & ENGINEERING TECHNOLOGY

Call : 08813907089  (24\*7 Support on Whatsapp)